VISTA HEMISPHERE SURVEY
DATA RELEASE 2

PROPOSAL ESO No.: 179.A-2010
PRINCIPAL INVESTIGATOR: Richard McMahon

Authors: R. McMahon, M. Banerji, N. Lodieu, Gonzalez, Kosporov for the VHS Collaboration.

Data Collection	<CollectionName>
Release Number	<Number/tag>
Data Provider	Richard McMahon, Manda Banerji, Nicholas Lodieu, Eduardo Gonzalez, Sergey Kosporov and the VHS collaboration
Date	?-10-2012

This above will be completed later when discussed with ESO. We need to agree consistent naming system for collections and release numbers for the VHS images, single band catalogues and bandmerged catalogue products.

1. Abstract

This is the second data release of science data products for the VISTA Hemisphere Survey (VHS). It contains data obtained during ESO observing periods 86 and 87 from Oct 1st 2010 to Sep 30th 2011.

The aim of the VISTA Hemisphere Survey (VHS; www.vista-vhs.org) is to carry out a near Infra-Red survey, which when combined with other VISTA Public Surveys will result in coverage of the whole southern celestial hemisphere (~20,000 deg^2) to a depth 30 times fainter than 2MASS/DENIS in at least two wavebands (J and K_s), with an exposure time of 60 seconds per waveband to produce median 5σ point source (Vega) limits of J = 20.2 and K_S = 18.1. In the South Galactic Cap, ~5000 deg^2 will be imaged deeper with an exposure time of 120 seconds and also including the H band producing median 5σ point limits of: J = 20.6; H = 19.8; K_s = 18.5. In this 5000deg^2 region of sky deep multi-band optical (grizY) imaging data will be provided by the Dark Energy Survey (DES). The remainder of the high galactic latitude (|b|>30°) sky will be imaged in YJHK for 60sec per band to be combined with ugriz waveband observations from the VST ATLAS survey.

The medium term scientific goals of VHS include:

- the discovery of the lowest-mass and nearest stars
- deciphering the merger history our own Galaxy via stellar galactic structure
- measurement of large-scale structure of the Universe out to z~1 and measuring the properties of Dark Energy
- discovery of the first quasars with z>7 for studies of the baryons in the intergalactic medium during the epoch of Reionization
- discovery of the most luminous quasars in the southern celestial hemisphere at all redshifts as probes of the IGM and the formation of the most massive supermassive black holes in the Universe

In addition the VHS survey will provide essential multi-wavelength support for the ESA Cornerstone missions; XMM-Newton, Planck, Herschel and GAIA.

2. Release content

The VHS survey data in this release consists of three survey components that have different OB structures.

- VHS DES: 120secs in J, H and K
- VHS ATLAS: 60secs in Y, J, H and K
- VHS GPS: 60secs in J and K

This release consists of observations obtained during ESO Period 86 and ESO Period 87; from Oct 1st 2010 to Sep 30th 2011. The previous VHS release (DR1) covered data up to the end of Period 85 on Sep 30th 2010. See Table 1a, 1b and 1c for a summary of the data products in each data release. The image products include pawprints, mosaiced tiles and confidence maps for both image products.

Table 1a: Summary of Releases: Images

ESO Period	Date range	Runs	Images		VDFS Pipeline version
			Pawprints	Tiles	
P84 (Dry Run)	Nov 2009 – Jan 2010	A	DR1	DR1	1.1
P85	Mar 2010 – Sep 2010	B	DR1	DR1	1.1
P86	Oct 2010 – Mar 2011	C	DR2	DR2	1.1
P87	Apr 2011 – Sep 2011	D	DR2	DR2	1.2

Table 1b: Summary of Releases: Single band catalogues

ESO Period	Date range	Runs	Single band catalogues		VDFS Pipeline version
			Pawprints	Tiles	
P84 (Dry Run)	Nov 2009 – Jan 2010	A	DR1	DR1	1.1
P85	Mar 2010 – Sep 2010	B	DR1	DR1	1.1
P86	Oct 2010 – Mar 2011	C	DR2	DR2	1.1
P87	Apr 2011 – Sep 2011	D	DR2	DR2	1.2

Table 1c: Summary of Releases: Band merged catalogues (in preparation)

ESO Period	Date range	Runs	Band merged catalogues	
			Pawprints	Tiles
P84 (Dry Run)	Nov 2009 – Jan 2010	A	-	DR2
P85	Mar 2010 – Sep 2011	B	-	DR2
P86	Oct 2011 – Mar 2011	C	-	DR2
P87	Apr 2011 – Sep 2011	D	-	DR2

In figure 1 we shows the RA, Dec distribution for all observations up to 30 Sep 2011. The figure shows data from both Data Release 1 and Data Release 2.

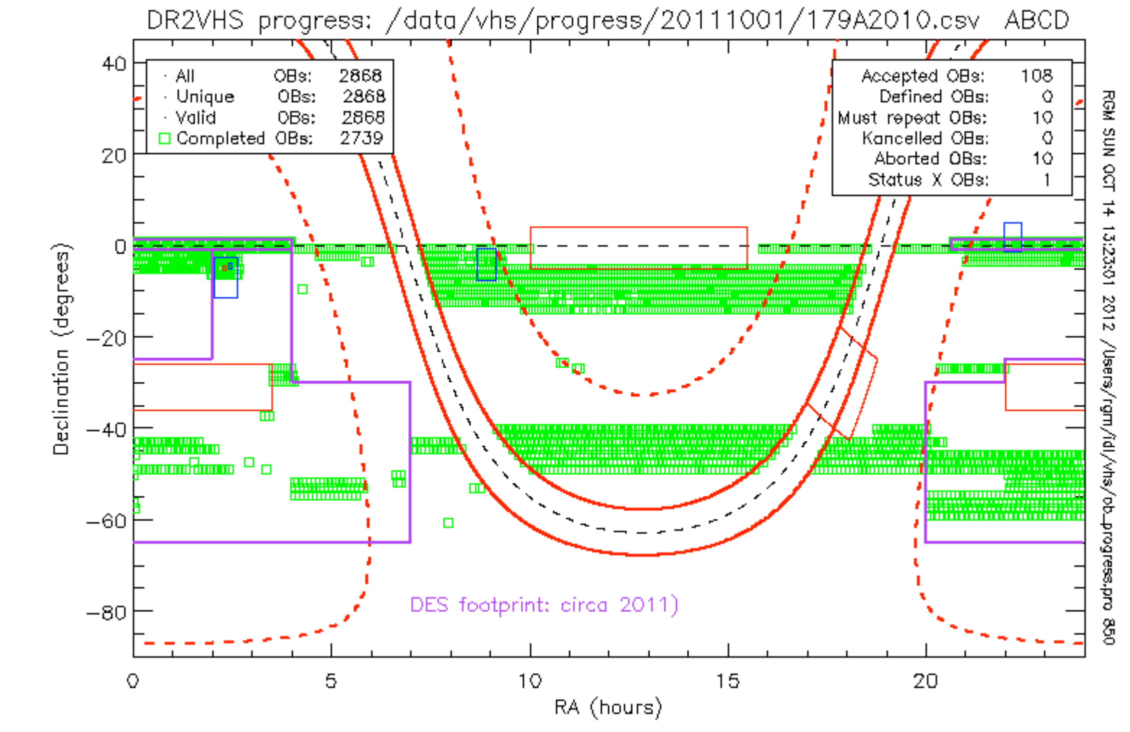

Figure 1: Sky coverage of the VHS survey in Data Release 1 + 2. The purple line shows the Dark Energy Survey (DES) footprint. The thin red solid lines show the nominal footprint of the VIKING survey which is avoided by VHS. The solid red lines show the galactic latitude= -5,5 and the bulge region of the VVV survey which is not covered by VHS. The black dashed lines show the celestial equator and the galactic equator. The dashed red lines are at galactic latitude -30 and 30.

Example colour-magnitude and colour-colour diagrams

Figures 2-4 show colour-magnitude and colour-colour diagrams for two typical fully reduced example high galactic latitude tiles. Some examples of problem tiles identified during VHS QC are shown in Figure 2. The blue points are objects classified as stars and the grey points are objects classified in K as non-stellar.

These QC diagrams demonstrate the precision of the photometry and star-galaxy separation. The J-K-v-K stellar locus clearly delineates the distinct disk dwarf and halo giant populations which show up as two separate populations with J-K<1.0. The non-stellar objects which are mainly external galaxies have J-K>1.0.

3. Release notes

Quality Control

The data processing of the science products released in this data release come for version 1.1 and 1.2 of the VISTA Data Flow System(VDFS) pipeline running at the Cambridge Astronomical Survey Unit(CASU). The change log for the pipeline is at:

http://casu.ast.cam.ac.uk/surveys-projects/vista/data-processing/version-log

Data obtained after the mirror coating intervention in Mar-April 2011 have been tagged as version 1.2, i.e., data obtained after 20110501. The changes between version 1.1 and 1.2 are as follows:

1. Addtional keyword NUMSTDS which stores number of 2MASS objects in the field of view of each chip or tile potentially usable for the astrometric solution.
2. Tiles now inherit the nightly photometric information from pawprints (keywords affected NIGHTNUM, NIGHTZPT, NIGHTZRR).
3. Provenance keyword values in tiles do not now have "tmp_" in the provenance information for the component filenames.
4. Added a GROUTED keyword to catalogues generated from tiles that have been grouted.
5. RADECSYS keyword changes. Primary extension remains FK5 while secondary extensions have the value ICRS added.
6. Added new keywords to the tile primary header: PAWMAGZP, PAWELLPT and PAWSEENG which summarize the median values of the zero point, ellipticity and seeing from originating pawprint images to aid in QC procedures.
7. The magnitude zero point error estimate for tiles is now calculated from the zero-point variation in the component pawprint images

Quality control consists of visual inspection of a subset of image and visual inspection of colour magnitude diagrams from all data. In addition the distribution of astrometric and photometric parameters are inspected. An independent check on the astrometry has been carried out via comparison with 2MASS using the VISTA Science Archive for a subset of the data. An independent check on the photometry has been carried by comparing the VHS Y, J, H and K photometry with the Y, J, H and K photometry from the UKIDSS survey.

Colour-magnitude and colour-colour plots as shown in Figure 2-4 are being produced for all paw-print and tile bandmerged catalogues. Figure 2 shows examples of version 1.0 VDFS data products that failed our QC. Figure 3 shows the VDFS version 1.1 data products for the same raw data and shows that the version 1.1 products now pass our image classification and photometric QC. Figure 4 shows data from the final VHS OB for Period 85 and Period 86 respectively.

Image quality
Figure 5 and 6 shows the distributions of the image quality in all wavebands for all VHS observations obtained in Periods 86+87. This plots contain repeat OBs and hence although the median value will be robust, poor quality data will be over represented. Figure 5 shows the measured seeing (FWHM) for stellar objects and Figure 6 shows the image ellipticity distribution. Visual inspection of the images with ellipticity > 0.15 is carried out. Some have double images whereas some may still be

useable. In Period 86 the ellipticity distribution has improved compared with Period 85. The measured image widths are around 0.1arcsecs larger in tiles compared with pawprints. This is under investigation but is likely to be due to astrometric uncertainties in the pawprints and the resampling and interpolation procedure used when combining pawprints images into tiles.

The medians of the pawprint seeing distributions show a wavelength dependence increasing from 0.89 arc seconds in K_S to 0.99 arc seconds in J. The ratio is consistent with a Kolmogorov $\lambda^{-1/5}$ wavelength dependence assuming a effective wavelengths of 2.149μm for K_S and 1.254μm for J. The Y band images have median seeing of 0.98 arc seconds. There is some evidence for an improvement in the seeing compated with DR1 which may be due to the use of higher AO priority.

The seeing distributions in J and Y have a significant tail to value that exceed out seeing limit of 1.4". Figure 7 shows the airmass distribution. This shows a tail above 1.5 airmasses which will contribute to the mediocre seeing tail.

Astrometry

Figure 8 shows the distribution of the World Cooordinate System (WCS) rms astrometric errors derived from 2MASS. The J and K bands have a tail to smaller values compared to Y and H, since there are J and K observations in regions of higher stellar density at lower galactic latitude. Figure 9 shows how the WCS rms is a function of the number of stars used in the fit. This shows the expected correlation between the number of stars and the rms residuals due to better determination of the WCS transformation. There is plateau in distribution in the J and K bands. The origin is under investigation. It could be a feature of sigma clipping of outliers. The higher surface density of 2MASS stars in J and K is due the lower latitude of some of the J and K observations compared with the Y and H observations which are only obtained at galactic latitude; |b| >30^{o} .

Table 2 VHS comparison with VLBI radio reference frame

Survey (number of sources)	sigma (Statistical)		Systematic uncertainty	
	RA	Dec	RA	Dec
VHS (563)	0.11"	0.09"	-0.011±0.005"	-0.051±0.004"
SDSS (2308)	0.05"	0.05"	0.006±0.001"	-0.003±0.001"
UKIDSS (599)	0.10"	0.09"	-0.031±0.004"	-0.068±0.004"

Figure 10 shows a comparison between VHS positions and the VLBI radio reference frame (http://astrogeo.org/vlbi/solutions/rfc_2012b). The results are summarized in Table 2 and compared with SDSS and UKIDSS. There is a statistically significant systematic error of 0.05 arc seconds in declination. This is consistent with expected proper motions of 2MASS stars (Roser et al, 2010, AJ, 139, 2440) due to the 10 year difference in epoch between 2MASS and VHS. Note this systematic error varies depending on direction in sky due to Solar motion with respect to average 2MASS reference star. Proper motions will be included in a future CASU processing based on UCAC4 or PPMXL (Roser et al, 2010, AJ, 139, 2440)

Zero-points, atmospheric transparency and sky brightness

Figure 11 and 12 shows the measured sky brightness and zero-point on tiles for all Period 86 VHS observations based on photometric calibration using 2MASS. There is a tail to bright magnitudes and ~10% have relative attenuation >0.2 magnitudes which is outside the ESO THIN constraint. Some of this may be due to the known degradation in the VISTA system throughput due to the degradation of the primary mirror reflectivity since the primary mirror was coated in September 2009.

Limiting magnitudes

Figure 13(a,b,c) shows the computed 5sigma point source limiting magnitudes for the 3 VHS survey components. Note the VHS DES component has exposure times of 120 seconds per band compared to 60 seconds for the other two components (GPS and ATLAS).

Large scale structure and artifacts

Figure 14 shows some the spatially dependent features of the VHS data based on a subset of this data release. In the three panels are show the patial distribution of all objects classified as stars on J and K in the RA range 140 to 250 degrees and Declination -4 to -15. From top:

1. All stars with J and K < 18;
2. as above stars with J-K>0.9;
3. as above but with J band average confidence > 95%.

The top panel shows an area of higher stellar density at the right hand side due to the proximity of the galactic centre. Apart from obvious gaps in the data due to coverage there are tile sized regions of lower surface density. These are due to tile with lower than average limiting magnitudes. The middle panel shows only stellar classified objects with J-K>0.9. There is evidence of tiles where there is an above average number of objects classified as stellar. This is due to poor seeing resulting in galaxies being classified as stellar. There is also a regular periodic pattern due the variable QE performance of part of detector 16 see:

http://casu.ast.cam.ac.uk/surveys-projects/vista/technical/known-issues

The lower panel shows a regular pattern at the edges of each time. This is due to the 50% exposure regions at the edges of each tile.

4. Data format

This data release consists of FITs format pawprint and tiles images and catalogues derived from both the pawprint and tile images. Further details about these data products can be obtained from the CASU website at

http://casu.ast.cam.ac.uk/surveys-projects/vista/technical

5. Acknowledgements

The acknowledgments to be included when using this data should include a reference to the survey description paper, McMahon et al in preparation.

Please also use the following statement of the form below in your articles when using these data. The ESO programme ID is mandatory.

"This paper uses data from the VISTA Hemisphere Survey ESO programme ID: 179.A-2010 (PI. McMahon)"

Based on data products from observations made with ESO Telescopes at the La Silla Paranal Observatory under programme ID *179.A-2010 (PI. McMahon)*

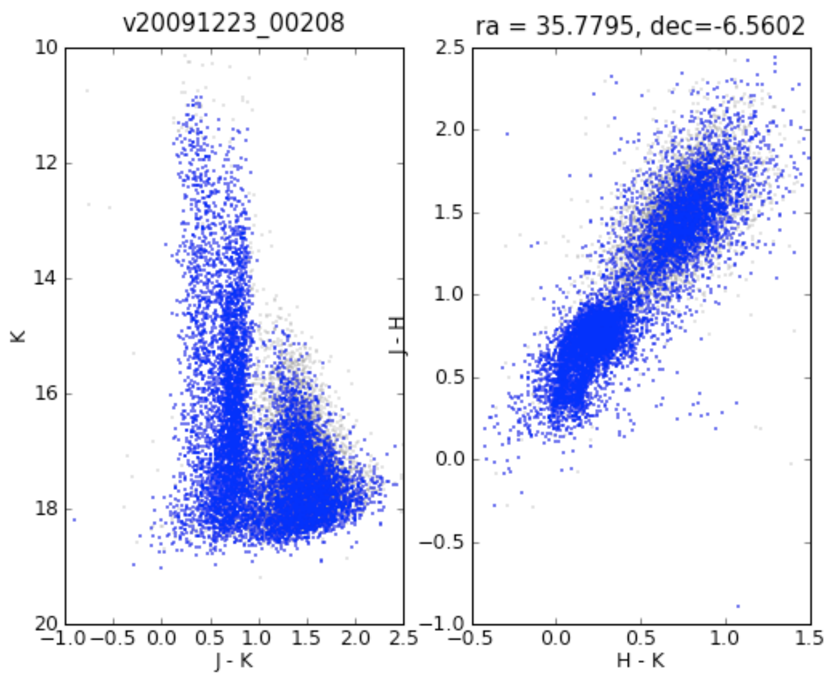

Figure 2(a): Version 1.0 data products showing QC problem with star-galaxy separation. Blue points are starlike objects; Grey points are non-stellar objects.

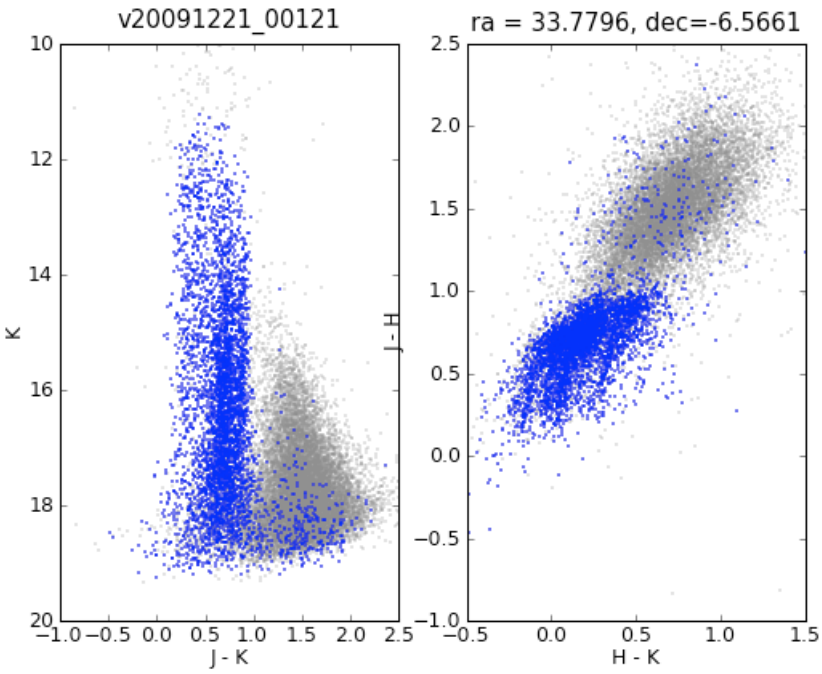

Figure 2(b): Version 1.0 data products showing QC problem with multiple offset stellar loci due to variable seeing causing spatially dependent aperture corrections in different pawprints. This is fixed via the grouting stage of the VDFS pipeline.

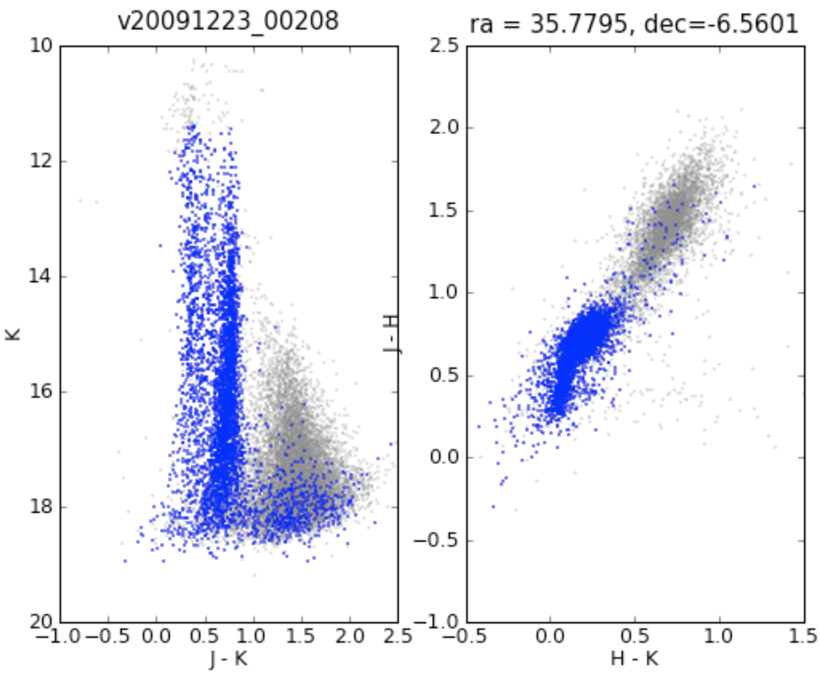

Figure 3(a): Version 1.1 data products for same observations as Figure 2(a) showing the improvement in star-galaxy separation for this OB. Blue points are starlike objects; Grey points are non-stellar objects

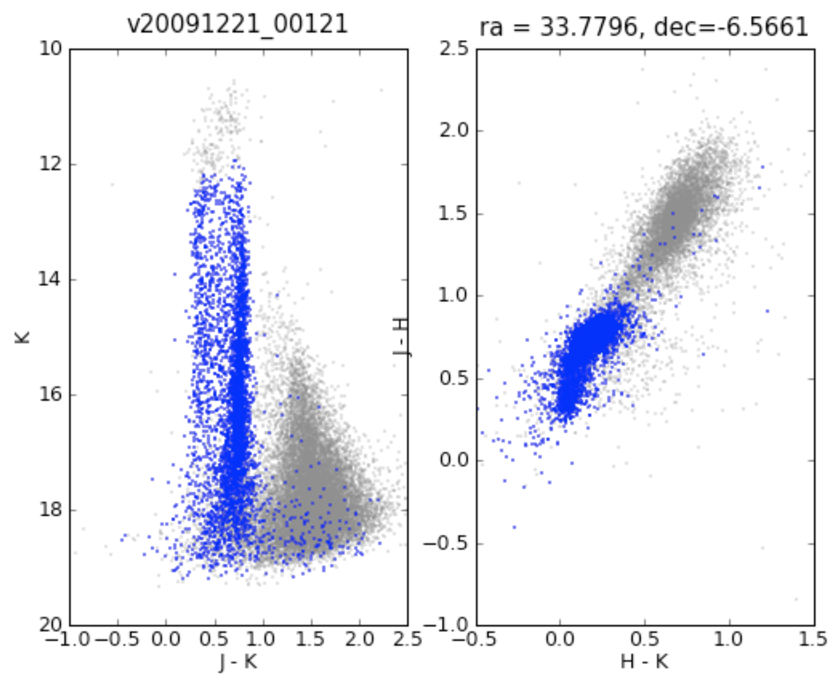

Figure 3(b): QC problem showing multiple offset stellar loci due to variable seeing causing spatially dependent aperture corrections in different pawprints.

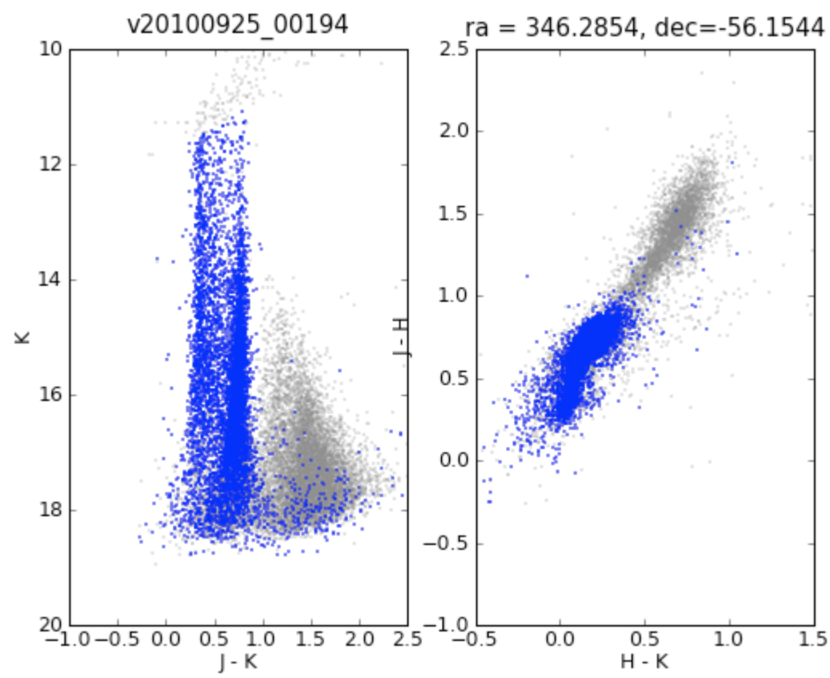

Figure 4(a): Version 1.1 data products for VHS final Period 85 OB acquired on 2010 Sep, 25th. Blue points are starlike objects; Grey points are non-stellar objects

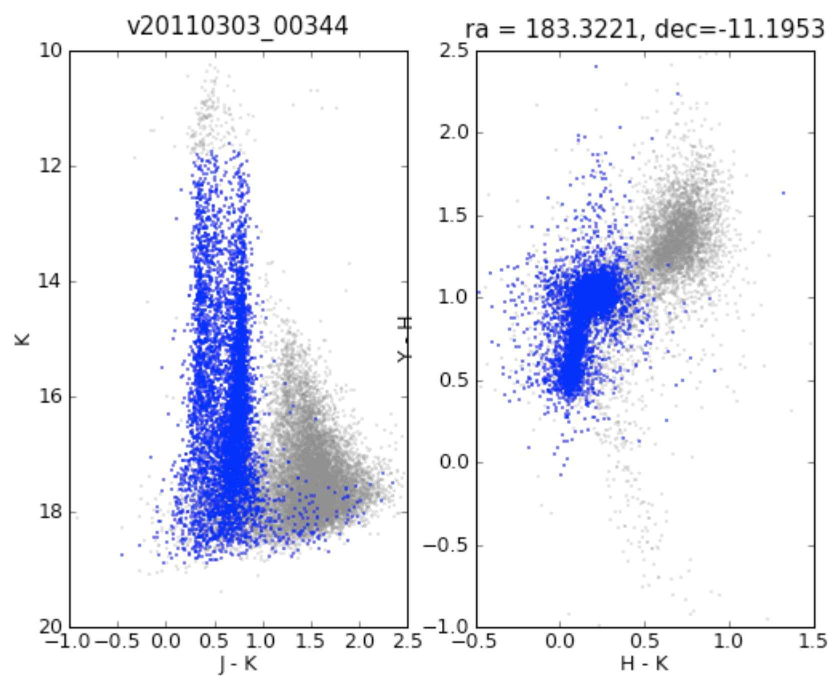

Figure 4(b): Version 1.1 data products for final VHS Period 86 OB acquired on 2011 March, 3rd; Note the right plot is H-K v Y-H whereas in other plots it is H-K v J-H

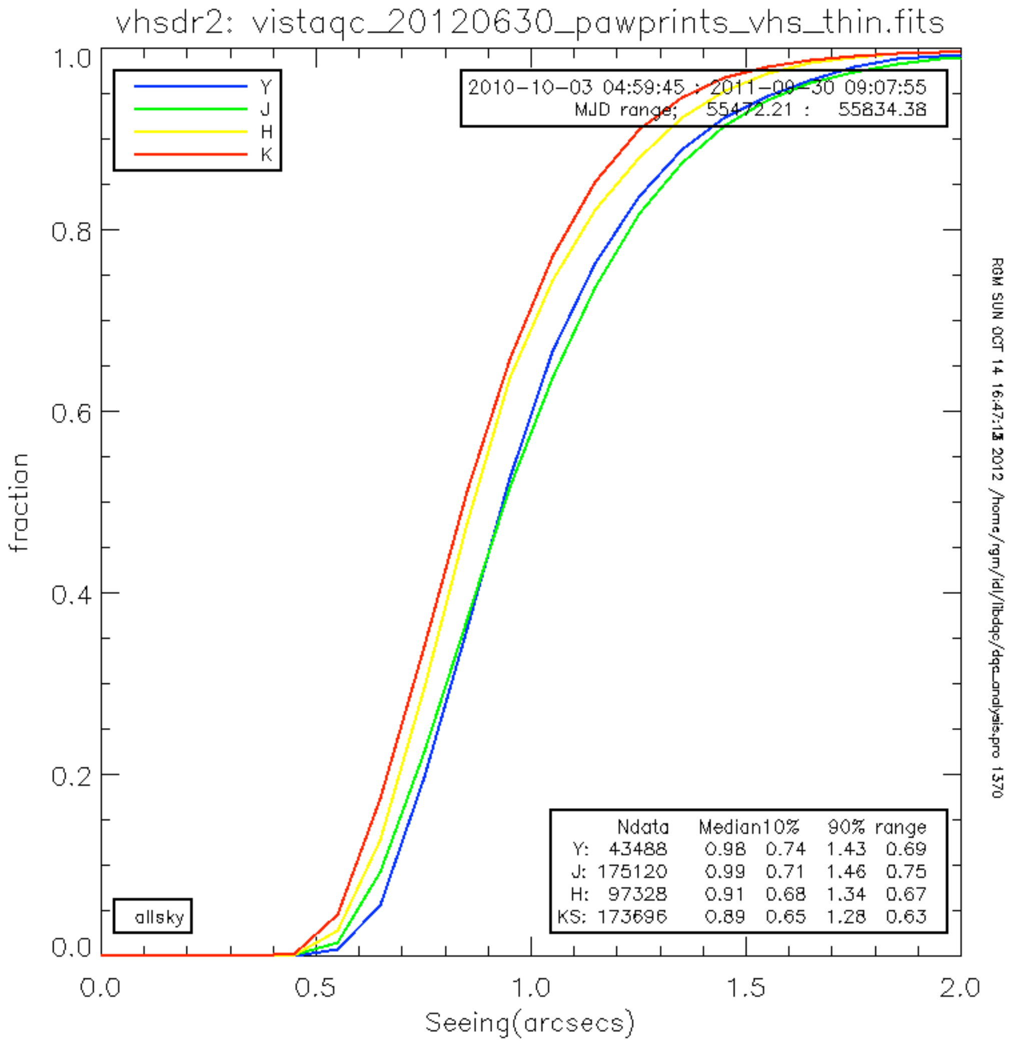

Figure 5a: Measured image seeing (stellar FWHM) on VHS pawprints observed during observing period 86 and 87 including rejected and repeated OBs.

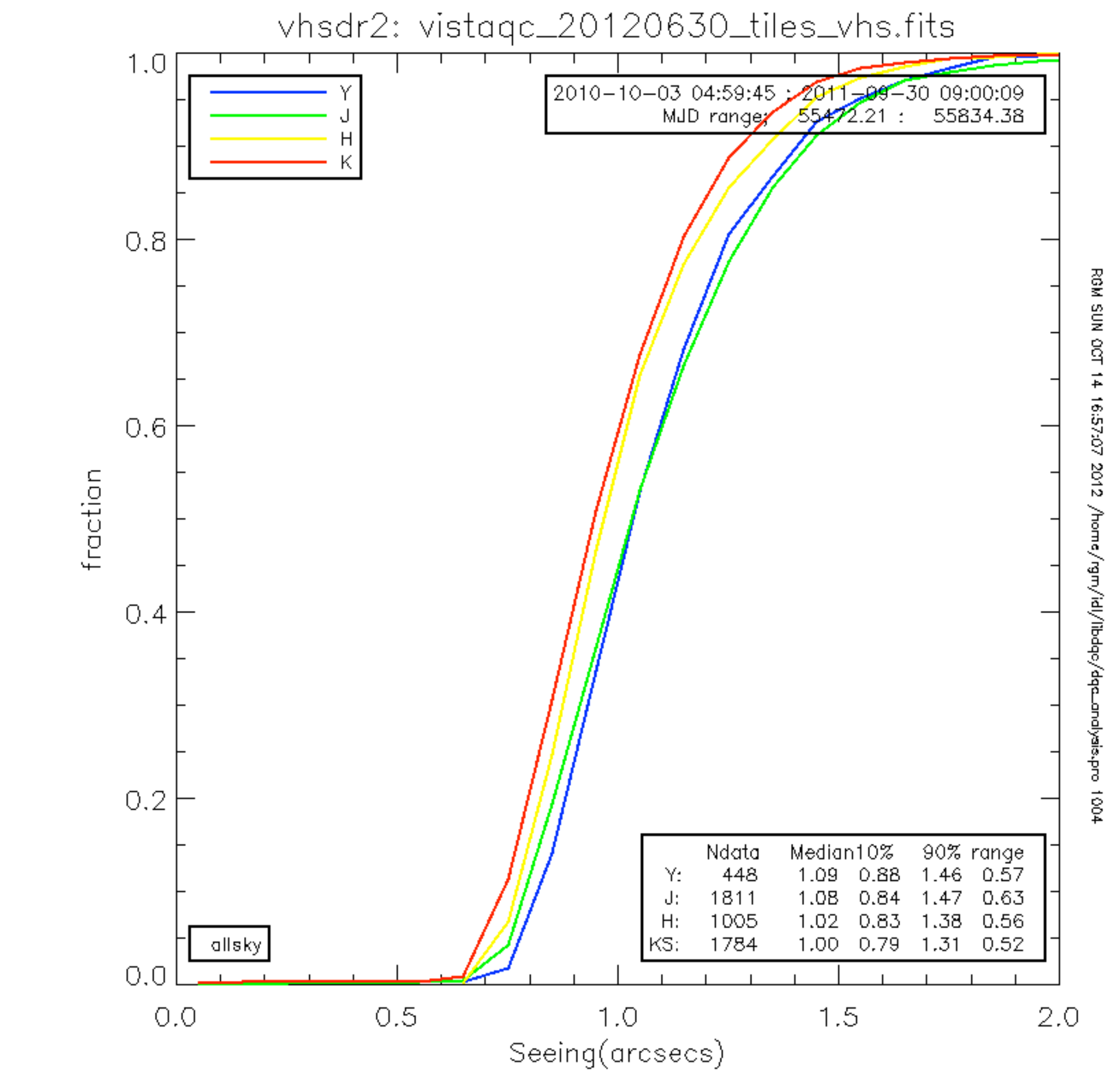

Figure 5b: Measured image seeing (stellar FWHM) on VHS tiles observed during ESO observing period 86 and 87 including rejected and repeated OBs.

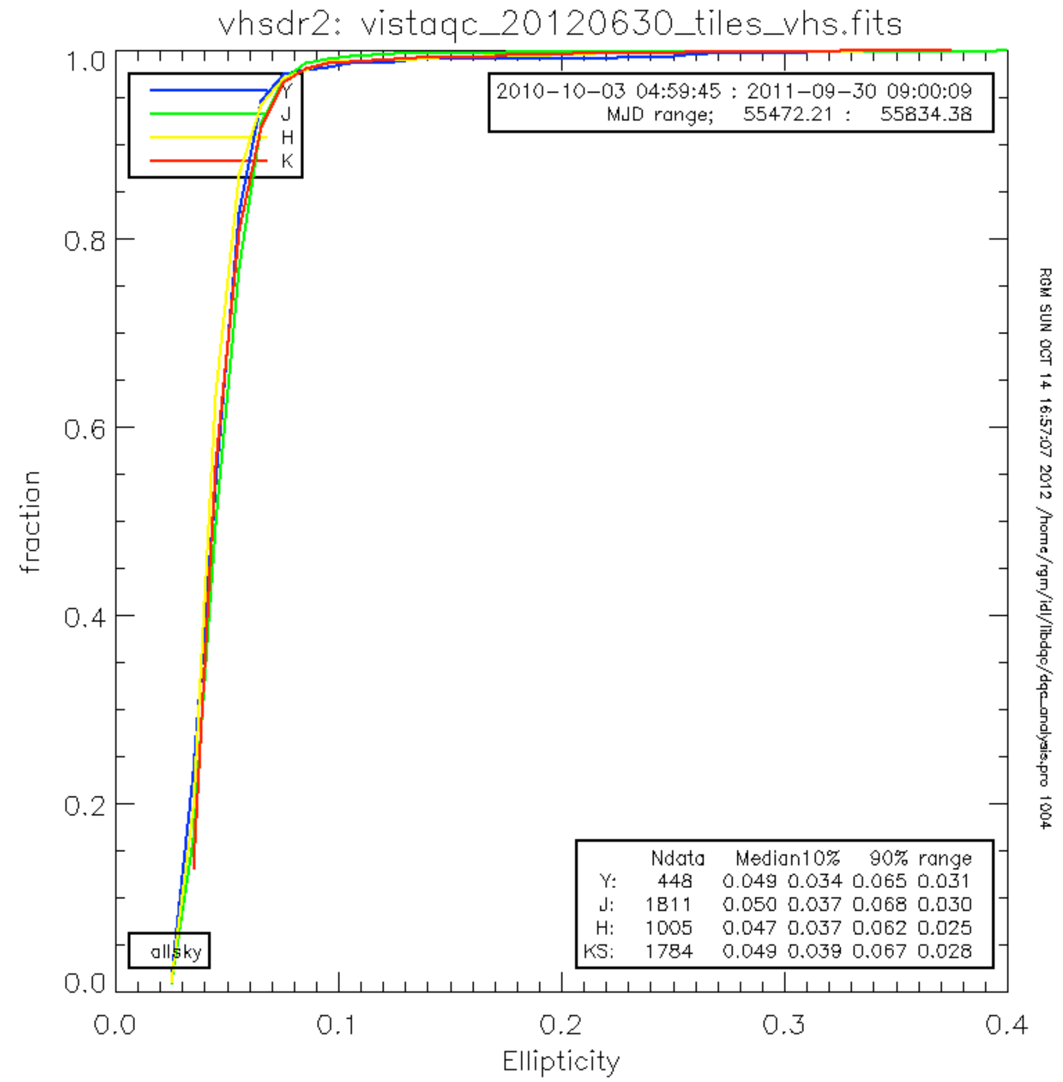

Figure 6: Measured stellar image ellipticity on all tiles for ESO Period 86 and 87 VHS observations including rejected and repeated OBs.

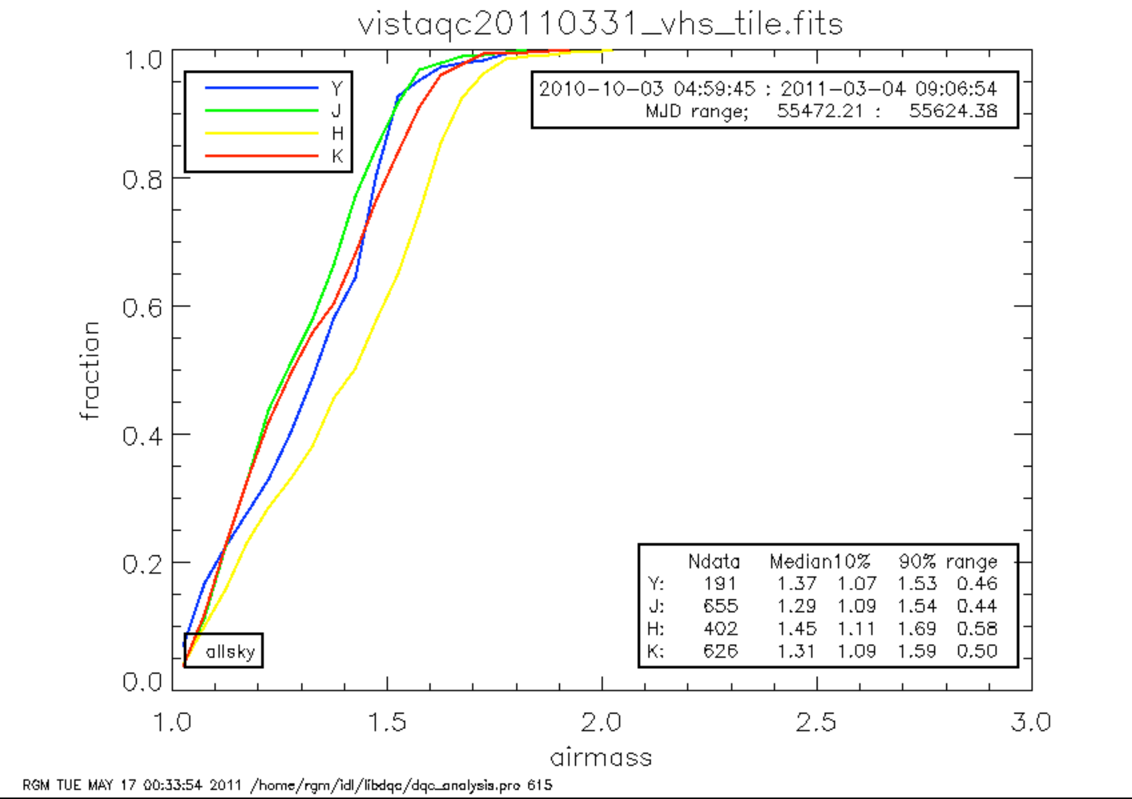

Figure 7: Airmass distribution for all Period 86 VHS observations i.e. includes rejected and repeated OBs.

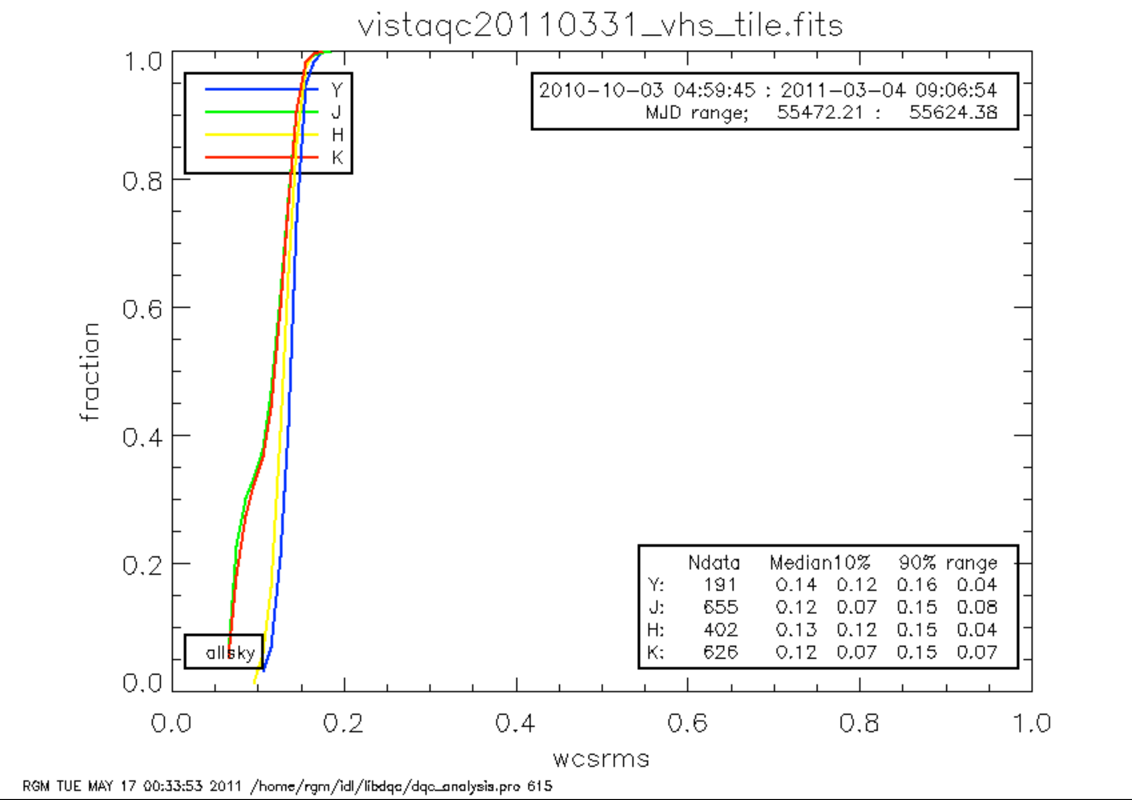

Figure 8: Distribution of the World Cooordinate System(WCS) rms astrometric errors for tiles. The J and K bands have a tail to smaller values compared to Y and H due to larger fraction of fields at low galactic latitude and hence more WCS 2MASS astrometric calibration stars.

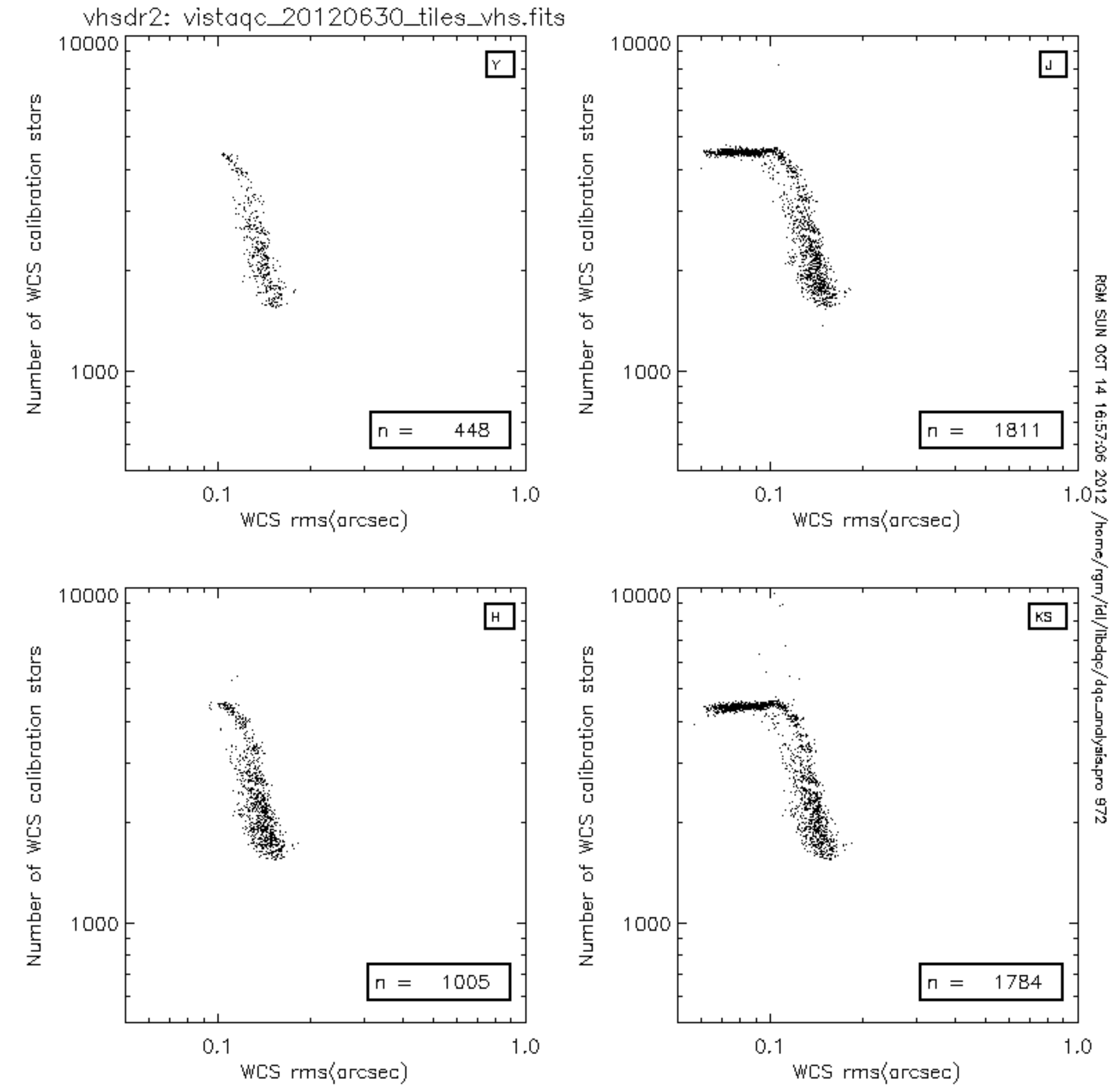

Figure 9: World Cooordinate System(WCS) rms astrometric errors versus number of 2MASS stars used for the WCS fits for tiles. This shows a correlation between the number of stars and the rms residual. There is plateau distribution in the J and K bands.

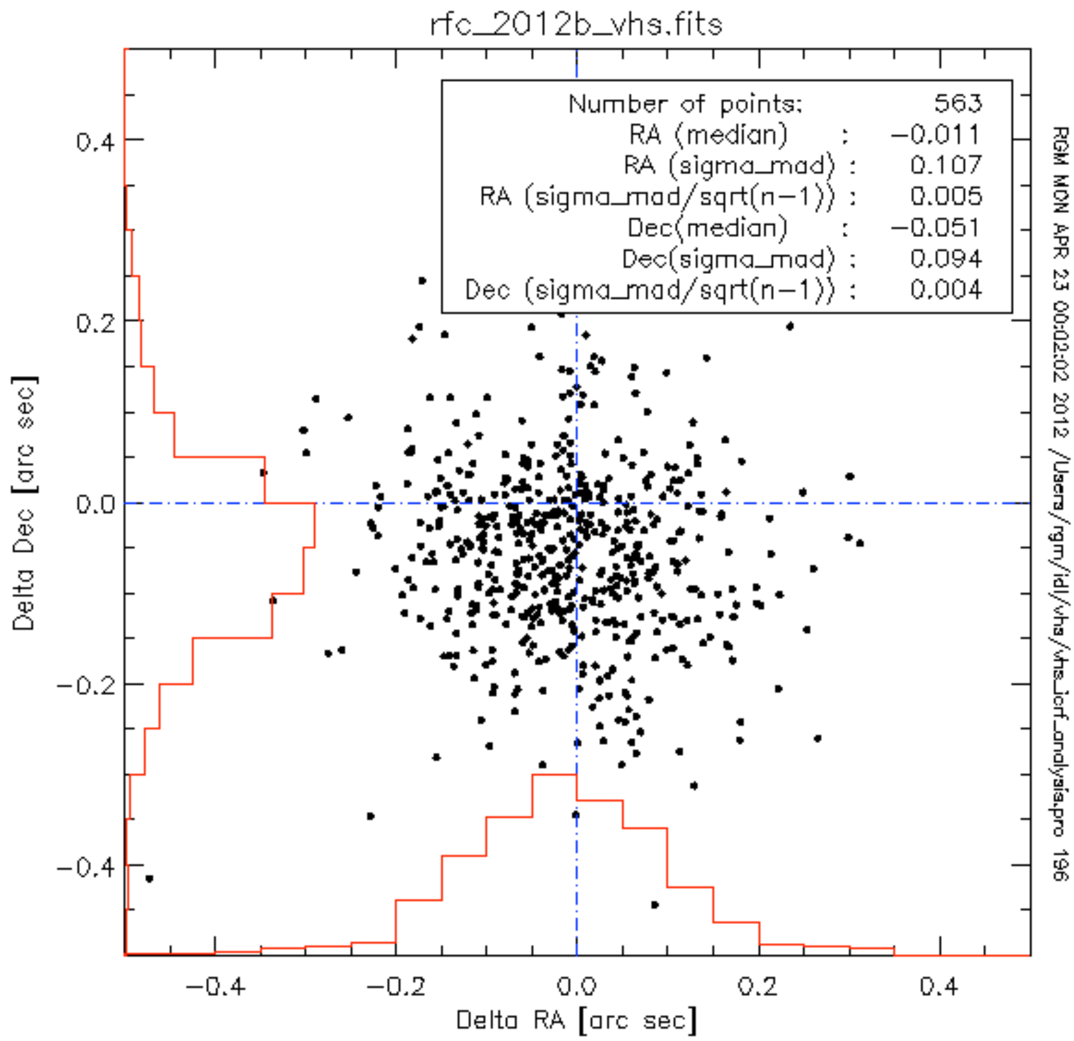

Figure 10: Comparison between VHS positions and the VLBI radio reference frame (http://astrogeo.org/vlbi/solutions/rfc_2012b).

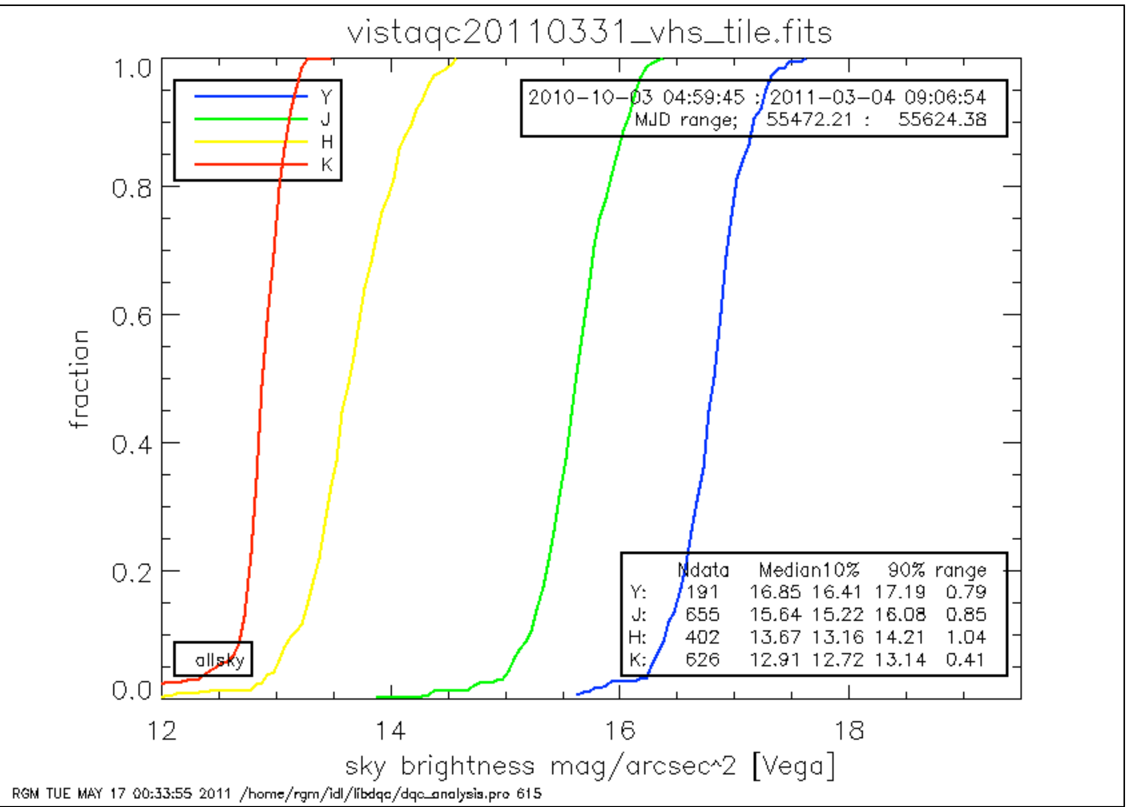

Figure 11: Measured sky brightness seeing on all VHS tiles for Period 86 observations. Note the tail to bright magnitudes that effects ~5% of observations.

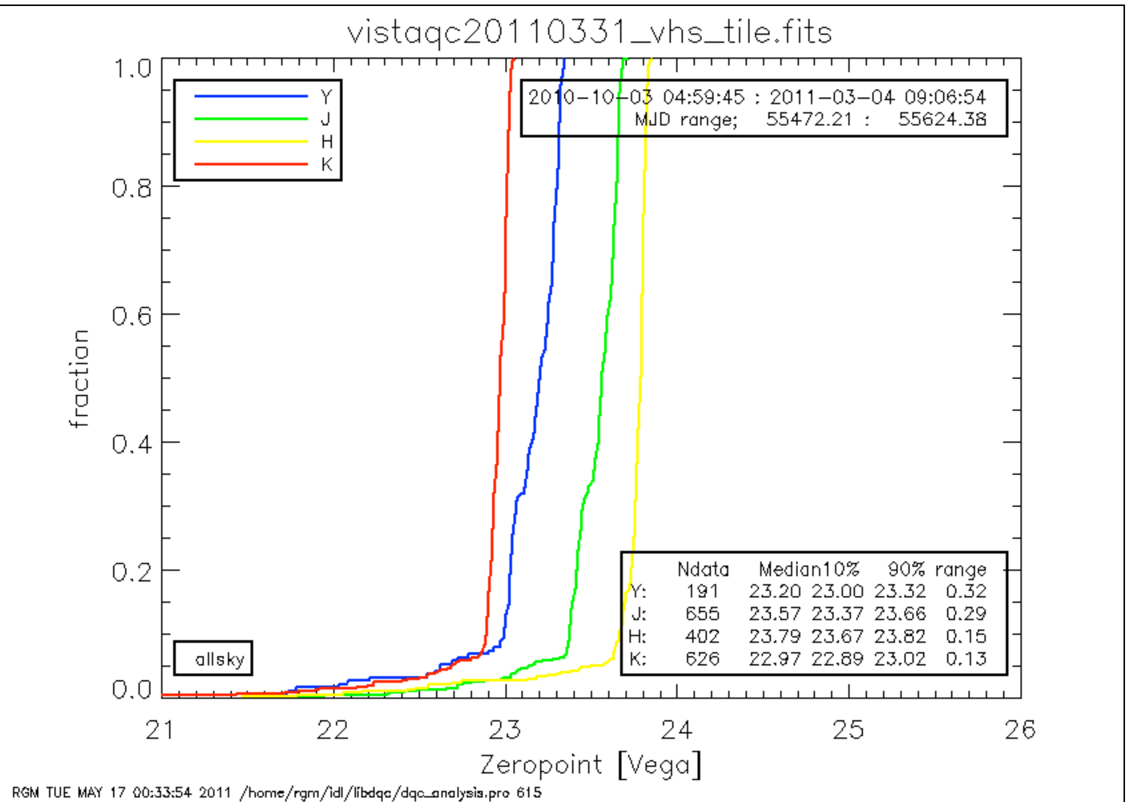

Figure 12: Measured zeropoint on tiles for all Period 86 VHS observations. Note the tail to bright magnitude. 5-10% have attenuation >0.2magnitudes.

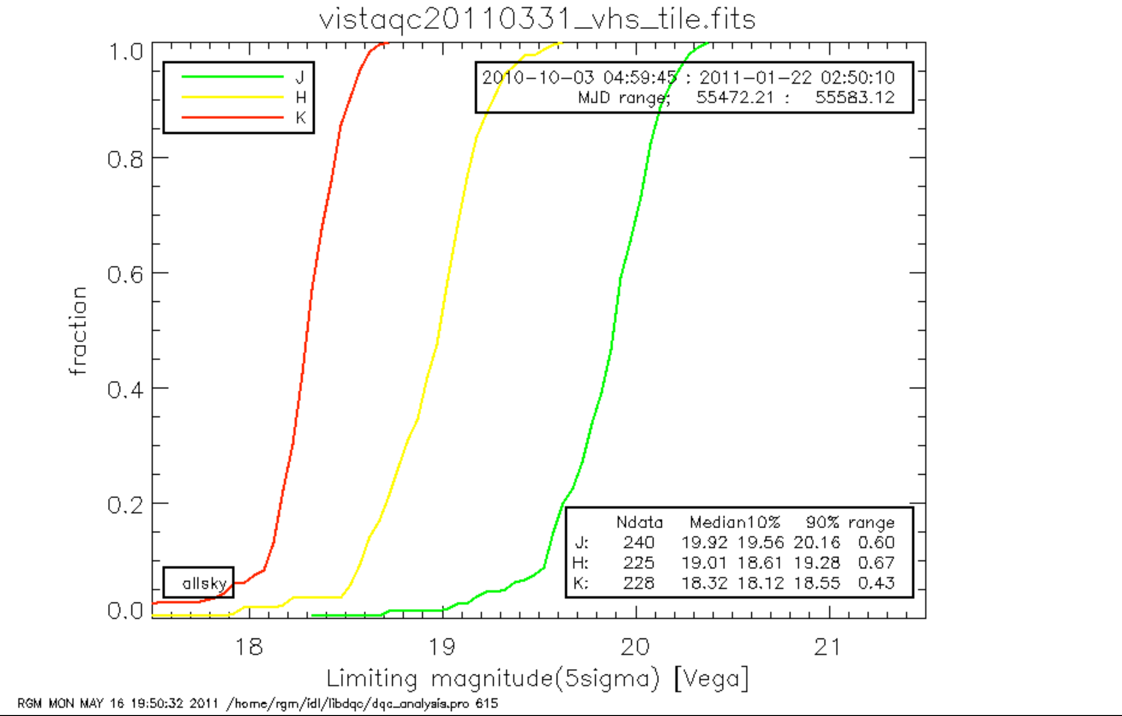

Figure 13(a): Limiting magnitudes for ESO Period 86 VHS DES component

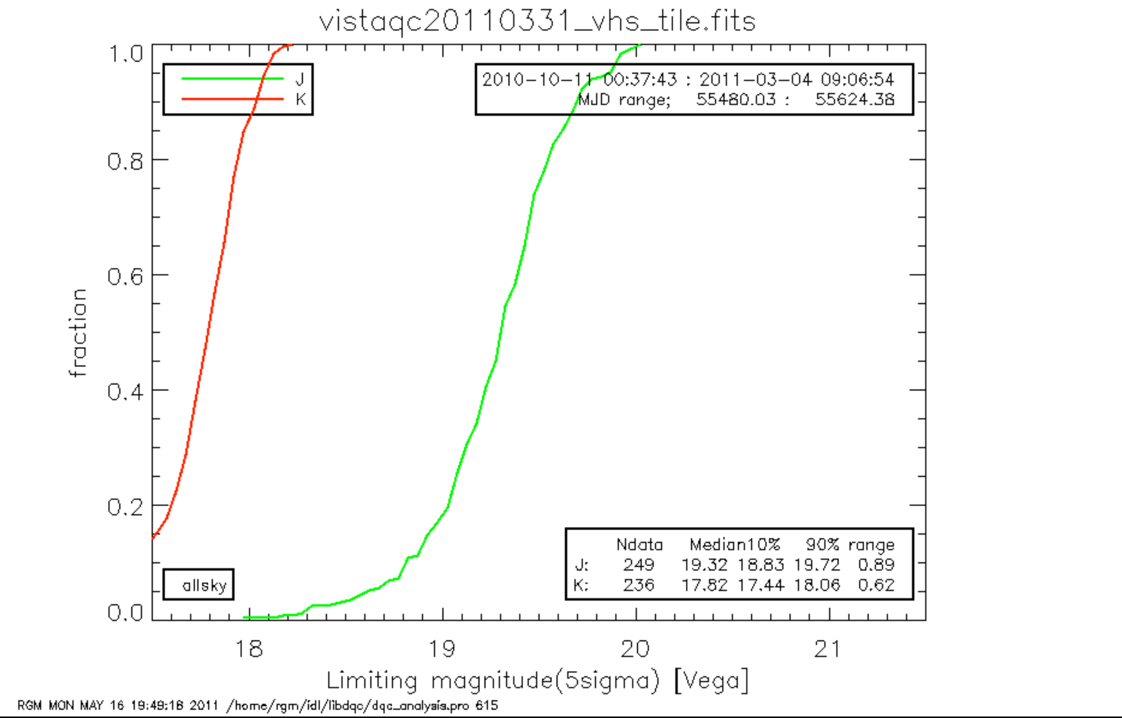

Figure 13(b): Limiting magnitude for ESO Period 86 VHS GPS component

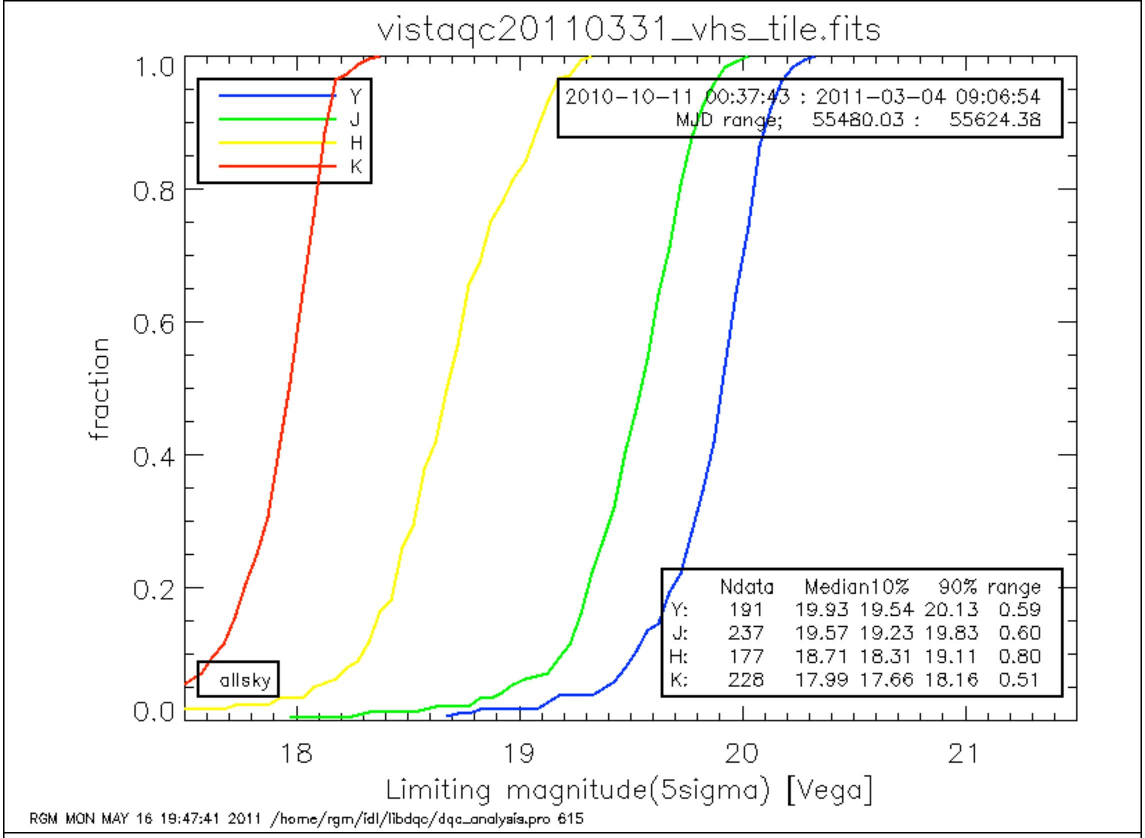

Figure 13c: Limiting magnitude for ESO Period 86 VHS ATLAS component

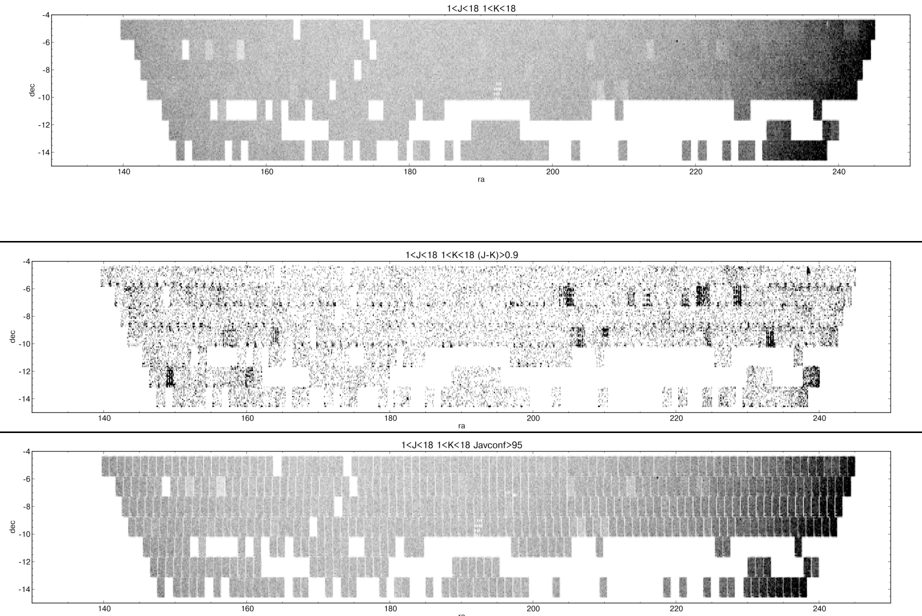

Figure 14: Spatial distribution of all objects classified as stars on J and K in the RA range 140 to 250 degrees and Declination -4 to -15. From top: All stars with J and K < 18; as above stars with J-K>0.9; as above but with J band average confidence > 95%.

Changelog:

oOo